Article

Cell Reports

A Mitochondria-Specific Isoform of FASTK Is Present In Mitochondrial RNA Granules and Regulates Gene Expression and Function

Graphical Abstract

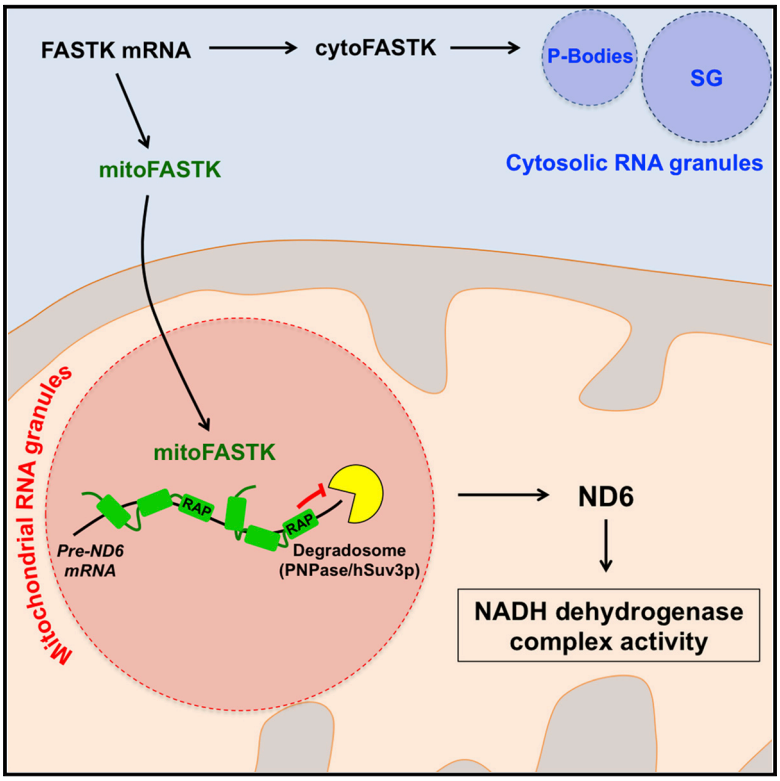

Highlights

- A mitochondrial isoform of FASTK co-localizes with mitochondrial RNA granules
- FASTK binds multiple sites along ND6 mRNA and its precursors
- FASTK modulates degradosome activity to generate mature ND6 mRNA
- ND6 mRNA levels and complex I activity are decreased in the absence of FASTK

Authors

Alexis A. Jourdain, Mirko Koppen, ..., Maria Simarro, Jean-Claude Martinou

Correspondence

jean-claude.martinou@unige.ch

In Brief

The mitochondrial genome is required for ATP production, but little is known about its expression. Jourdain et al. report that FASTK localizes to mitochondrial RNA granules and is essential for ND6 mRNA biogenesis and complex I activity via a mechanism of mRNA 3′ end processing in human mitochondria.

Jourdain et al., 2015, Cell Reports *10*, 1110–1121
February 24, 2015
http://dx.doi.org/10.1016/j.celrep.2015.01.063

OPEN ACCESS
CellPress

Cell Reports
Article

A Mitochondria-Specific Isoform of FASTK Is Present In Mitochondrial RNA Granules and Regulates Gene Expression and Function

Alexis A. Jourdain,[1] Mirko Koppen,[1,6] Christopher D. Rodley,[1] Kinsey Maundrell,[1] Naïg Gueguen,[2] Pascal Reynier,[2] Adela M. Guaras,[3] José A. Enriquez,[3] Paul Anderson,[4] Maria Simarro,[4,5] and Jean-Claude Martinou[1,*]
[1]Department of Cell Biology, University of Geneva, 30 quai Ernest-Ansermet, 1211 Genève 4, Switzerland
[2]UMR CNRS 6214 - INSERM 1083, Département de Biochimie et Génétique, CHU d'Angers, 4 rue Larrey, 49933 Angers Cedex, France
[3]Centro Nacional de Investigaciones Cardiovasculares Carlos III, Melchor Fernández Almagro 3, 28029 Madrid, Spain
[4]Division of Rheumatology, Immunology and Allergy, Brigham and Women's Hospital, One Jimmy Fund Way, Smith 652, Boston, MA 02115, USA
[5]Departamento de Microbiologia, Facultad de Medicina, Edificio de Ciencias de la Salud, Avda ramon y Cajal 7, Valladolid 47005, Spain
[6]Present address: STADA Arzneimittel AG, Stadastrasse 2-18, 81118 Bad Vilbel, Germany
*Correspondence: jean-claude.martinou@unige.ch
http://dx.doi.org/10.1016/j.celrep.2015.01.063

SUMMARY

The mitochondrial genome relies heavily on post-transcriptional events for its proper expression, and misregulation of this process can cause mitochondrial genetic diseases in humans. Here, we report that a novel translational variant of Fas-activated serine/threonine kinase (FASTK) co-localizes with mitochondrial RNA granules and is required for the biogenesis of ND6 mRNA, a mitochondrial-encoded subunit of the NADH dehydrogenase complex (complex I). We show that ablating FASTK expression in cultured cells and mice results specifically in loss of ND6 mRNA and reduced complex I activity in vivo. FASTK binds at multiple sites along the ND6 mRNA and its precursors and cooperates with the mitochondrial degradosome to ensure regulated ND6 mRNA biogenesis. These data provide insights into the mechanism and control of mitochondrial RNA processing within mitochondrial RNA granules.

INTRODUCTION

Mitochondria play a central role in the production of ATP through oxidative phosphorylation, a process that requires five large protein complexes (complex I–V) located at the inner mitochondrial membrane. Close to 100 proteins participate in the respiratory chain, and whereas most of these are encoded in the nucleus and imported into mitochondria from the cytoplasm, 13 proteins are encoded within the mitochondrial genome. In addition to the protein components of the respiratory chain, the mitochondrial genome also encodes two rRNAs and 22 tRNAs required for translation of the mitochondrial-encoded proteins. Mutations in many of the genes encoding these proteins have been associated with severe human pathologies for which no cure currently exists (Chinnery and Hudson, 2013). Mitochondrial transcription is initiated from the "D-loop" region of the mitochondrial genome and gives rise to long polycistronic precursor transcripts that span almost the entire mitochondrial genome (reviewed in Hällberg and Larsson, 2014). After transcription, the primary transcripts are processed to yield individual mature RNAs, in most cases by removal of flanking tRNAs according to the tRNA punctuation model (Ojala et al., 1981). However, this model does not completely explain how every mRNA is excised from the polycistronic transcript because atypical junctions exist that lack flanking tRNAs. Four such atypical junctions are found in the human mitochondrial genome: (1) at the 3′ end of the COX1 mRNA; (2) between the ATP8/6 and COX3 mRNAs; (3) between the ND5 and CYB mRNAs; and (4) at the 3′ end of ND6 mRNA (for a map of the mitochondrial genome, see Figures 6C and S5A). The heavy-strand-encoded mitochondrial RNAs exist predominantly as mono- or bicistronic RNAs, whereas ND6 mRNA, the only mRNA encoded by the light strand, is present at steady state in both the mature form of 1.0–1.1 kb and as several higher-molecular-weight precursor RNAs called RNA1–3 (Ojala et al., 1981). The wide variation in steady-state levels of the mature mitochondrial RNAs that originate from both the heavy- and light-strand polycistronic precursors underlines the importance of post-transcriptional regulatory mechanisms in controlling the stability and metabolism of the individual mitochondrial transcripts (Temperley et al., 2010; Rackham et al., 2012).

We and others have recently observed the presence of RNA granules within mitochondria (Antonicka et al., 2013; Borowski et al., 2013; Jourdain et al., 2013). These mitochondrial RNA granules have been shown to be associated with proteins that are functionally linked to the post-transcriptional regulation of mitochondrial RNAs, such as RNase P, RNase Z, and GRSF1 involved in RNA processing (Antonicka et al., 2013; Jourdain et al., 2013; Bogenhagen et al., 2014); the mitochondrial polynucleotide phosphorylase (PNPase)-hSuv3p helicase complex, or mitochondrial degradosome known to degrade the so-called

"mirror" RNAs complementary to the mitochondrial genes (Szczesny et al., 2010; Borowski et al., 2013); the mitochondrial poly(A) polymerase (Wilson et al., 2014); and RNA methyltransferases (Vilardo et al., 2012; Jourdain et al., 2013; Lee et al., 2013). The presence of these enzymes in RNA granules therefore suggests a role for this novel mitochondrial compartment in post-transcriptional regulation of mitochondrial RNA expression and turnover.

In an effort to identify new mitochondrial RNA granule components, the protein FASTK (Fas-activated serine/threonine kinase) caught our attention because (1) it is likely to be mitochondrial (Pagliarini et al., 2008), (2) it binds RNA (Castello et al., 2012), and (3) it is known to be a component of cytosolic RNA granules (Kedersha et al., 2005). FASTK had initially been described as a kinase activated by Fas signaling (Tian et al., 1995), but the arguments in favor of this activity have been recently questioned and this protein should no longer be considered as a kinase (Simarro et al., 2007). We now know that FASTK regulates alternative splicing in the nucleus and co-localizes with stress granules and processing bodies (P-bodies), two types of cytosolic RNA granules (Kedersha et al., 2005; Simarro et al., 2007). FASTK knockout ($FASTK^{-/-}$) mice have been generated, and analysis of their immune system revealed that FASTK promotes neutrophil recruitment and inflammation (Simarro et al., 2010a). Which of the putative functions and sites of action of FASTK accounts for the phenotype of $FASTK^{-/-}$ mice is currently unknown.

In humans, FASTK is the founding member of a family of proteins, which, in addition to FASTK itself, contains five additional members called FASTKD1–FASTKD5 (Figure S1A). All FASTKDs are characterized by an N-terminal mitochondrial-targeting signal (Simarro et al., 2010b) and the presence of three conserved but largely uncharacterized domains called FAST_1, FAST_2, and RAP (Figure S1A). According to homology predictions, the ~60-amino-acid RAP domain is likely to bind RNA (Lee and Hong, 2004), and indeed, all members of the FASTK family have recently been found in screens for RNA-binding proteins (Baltz et al., 2012; Castello et al., 2012; Wolf and Mootha, 2014). The function of the FASTK family members in mitochondria has not been studied in detail, although pioneering work from Simarro et al. (2010b) has shown that FASTKD3 is required for mitochondrial oxygen consumption. Interestingly, FASTKD2 has been found to be mutated in two siblings from a consanguineous Bedouin family, leading to infantile mitochondrial encephalomyopathy (Ghezzi et al., 2008). The precise mechanism underlying the pathology associated with the FASTKD2 mutation remains to be established.

Here, we investigate the mitochondrial localization and mechanism of action of FASTK. We report that, in addition to its previously reported dual cytosolic and nuclear localization, FASTK is also able to enter the mitochondria by virtue of a cryptic mitochondrial-targeting sequence that initiates at an alternative internal methionine. We show that FASTK is concentrated in mitochondrial RNA granules and that it functions to regulate specifically expression of the ND6 mRNA, the only protein-coding sequence located on the light-strand transcript. We show that FASTK binds the light-strand precursor RNA at multiple sites both within and downstream of the ND6-coding sequence and that, together with the mitochondrial degradosome, it participates in generating the mature form of the ND6 mRNA. In the absence of mitochondrial FASTK, the ND6 mRNA is undetectable, resulting in decreased complex I activity in FASTK-depleted cells and mice.

RESULTS

A Cryptic Mitochondrial-Targeting Signal in FASTK

The subcellular localization of FASTK in 143B cells and mouse embryonic fibroblasts (MEFs) was investigated by immunoblot analysis. Two bands of ~60 kDa and ~50 kDa could be detected (Figures 1A and 1B), and both bands were absent in extracts from 143B cells expressing an shRNA against FASTK or in $FASTK^{-/-}$ MEFs (Figures 1A and 1B). Subcellular fractionation experiments indicated that the long form of FASTK was enriched in the cytosolic and nuclear fractions, whereas the short form was enriched in mitochondria (Figure 1C). FASTK apparently migrated more slowly in the nucleus, which could correlate with phosphorylation of the protein (Tian et al., 1995), though this was not investigated further in this study. In mitochondria, FASTK was localized to the matrix as determined by the proteinase K accessibility test and is most likely attached to the inner membrane because it remained associated with the membrane fraction after alkali treatment (Figures 1D and 1E). Immunocytological staining of C-terminal HA-tagged FASTK (FASTK-HA) using an antibody directed against the HA tag confirmed the tripartite localization of FASTK in the nucleus, cytosol, and mitochondria and revealed the presence of foci in the organelle (Figures 1F and 1G, left panel) reminiscent of the mitochondrial RNA granules described previously (Jourdain et al., 2013). Importantly, the two-band pattern of FASTK seen by western blotting was also observed when FASTK-HA was expressed exogenously (Figure 1F), indicating that a single FASTK mRNA encodes two protein isoforms with different subcellular localizations (Figure 1H).

Several post-transcriptional mechanisms are able to generate alternative protein isoforms from a single mRNA transcript. In the case of FASTK, we were intrigued by the conserved in-frame ATG at position 103 coding for methionine 35 (M35) (Figures 1H and S2A), because alternative translation initiation sites have previously been shown to target proteins to different cellular compartments, including mitochondria (Kazak et al., 2013). To investigate the presence of an alternative start site in FASTK, we mutated the second ATG (FASTK-HA M35G) and observed that this mutation completely abolished the mitochondrial localization of the protein without affecting its cytosolic or nuclear localization (Figure 1G, center panel). Furthermore, immunoblot analysis revealed only the long form of FASTK, whereas the short form was completely absent (Figure 1F). To confirm these data directly, we constructed the N-terminally truncated isoform of FASTK, which initiates at M35 (FASTK-HA Δ1–34). After transfection into 143B cells, we found that FASTK-HA Δ1–34 was localized exclusively in mitochondria (Figure 1G, right panel). Immunoblot analysis of these cells showed that the protein co-migrated with the short form of endogenous FASTK (Figure 1F). These findings suggested that a cryptic mitochondrial-targeting sequence (MTS) may lie downstream of M35. To test this, we fused the first 25 residues following M35

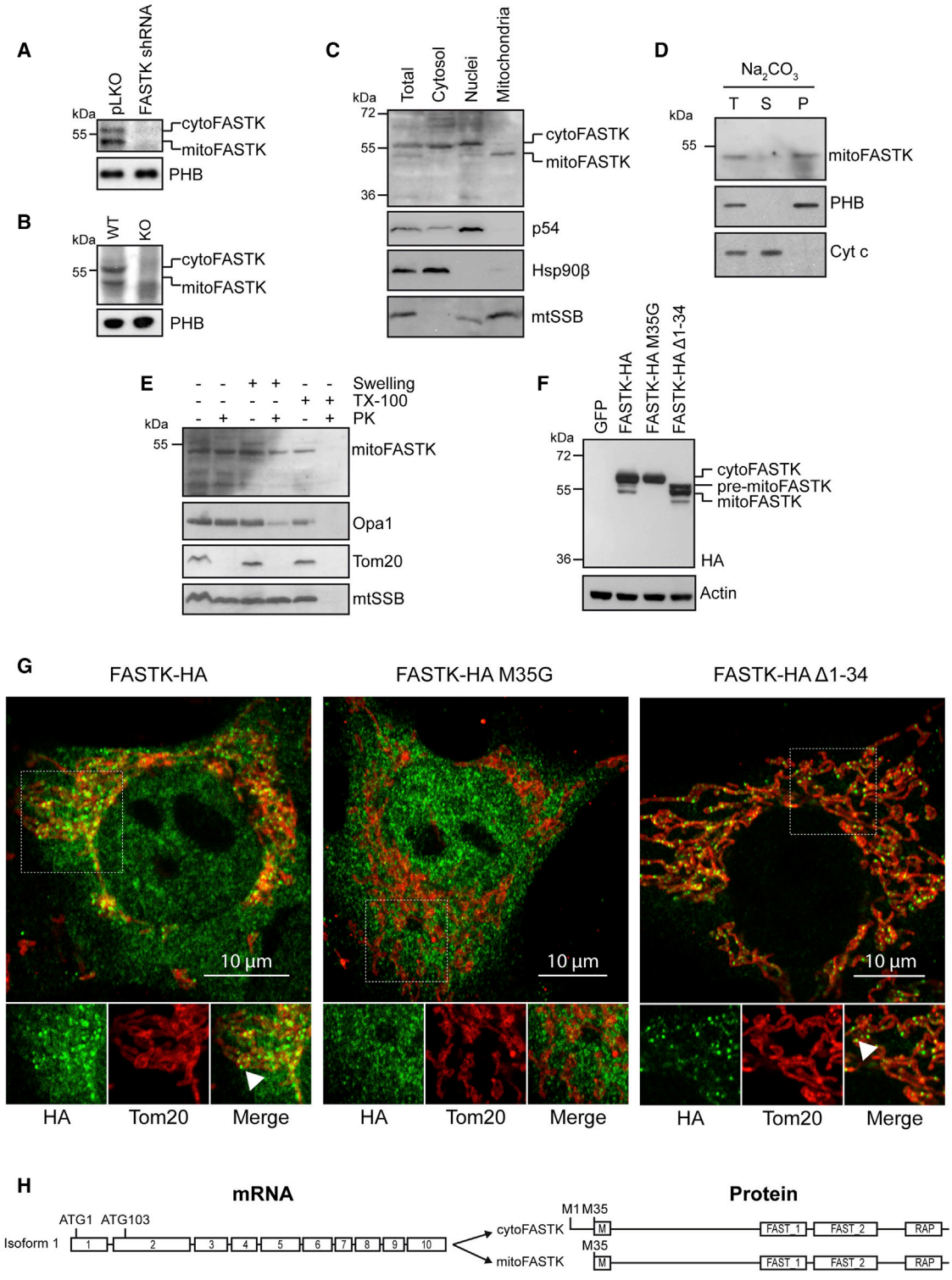

Figure 1. FASTK Is a Mitochondrial Protein

(A) Immunoblot analysis of 143B cells stably expressing an shRNA directed against FASTK. Membranes were probed with anti-FASTK and reprobed with anti-PHB to verify equal sample loading.

(B) Immunoblot analysis of FASTK$^{+/+}$ (WT) and FASTK$^{-/-}$ (KO) MEFs. Membranes were probed as in (A).

(legend continued on next page)

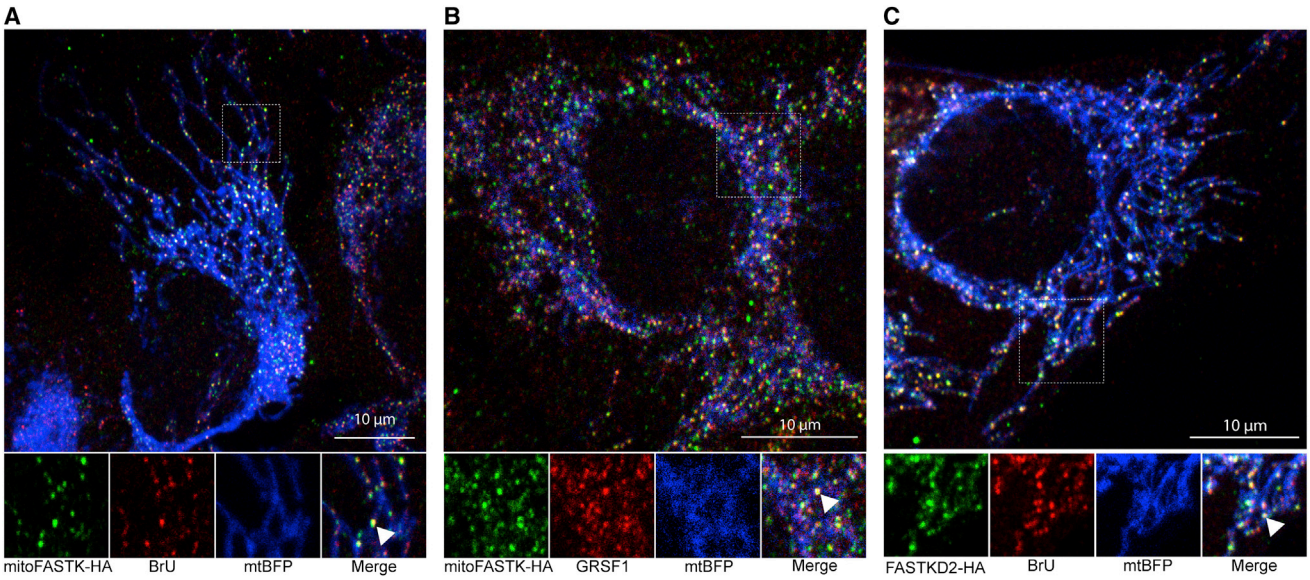

Figure 2. FASTK Co-localizes with Mitochondrial RNA Granules

(A) Confocal microscopy analysis of 143B cells stably expressing mitoFASTK-HA and mitoBFP, a mitochondrial-targeted version of the blue fluorescent protein. Cells were incubated with 5 mM BrU for 1 hr before immunolabelling with anti-HA and anti-BrU/BrdU antibodies. Arrowhead, mitochondrial RNA granule.

(B) Confocal microscopy of 143B cells stably expressing mitoFASTK-HA and mitoBFP. Cells were immunolabelled with anti-HA and anti-GRSF1 antibodies. Arrowhead, mitochondrial RNA granule.

(C) Confocal microscopy analysis of 143B cells stably expressing FASTKD2-HA and mitoBFP. Cells were incubated with 5 mM BrU for 1 hr before immunolabelling with anti-HA and anti-BrU/BrdU antibodies. Arrowhead, mitochondrial RNA granule.

to GFP (FASTK 35-60-GFP) and observed that this sequence was sufficient to target GFP to mitochondria (Figure S2B). Additional confirmation was obtained by mitochondrial import studies in which we showed that in-vitro-translated FASTK-HA Δ1–34, but not FASTK-HA M35G, could be imported into isolated 143B mitochondria in a membrane-potential-dependent manner (Figure S2C). Taken together, these data demonstrate that FASTK can be translated from either the first initiation codon (Figure 1H) to provide the cytosolic and nuclear forms of the protein (cytoFASTK) or from M35 to generate a shorter form that is targeted to mitochondria (mitoFASTK).

FASTK Co-localizes with Mitochondrial RNA Granules

As mentioned above, the analysis of FASTK-HA by immunofluorescence using an antibody to the HA tag revealed the presence of mitochondrial-RNA-granule-like structures in the mitochondria of transfected cells (Figure 1G, left panel), and this granular distribution was also seen in cells expressing mitoFASTK-HA (Figure 1G, right panel). In previous studies, we and others have shown that mitochondrial RNA granules accumulate newly synthesized RNA and can be observed by BrU labeling (Iborra et al., 2004; Jourdain et al., 2013), and we thus assessed whether mitoFASTK-HA co-localized with BrU-labeled granules in 143B cells. In cells stably expressing mitoFASTK-HA, we found that 92% (n = 100) of foci containing FASTK were positive for BrU (Figure 2A) and that mitoFASTK also co-localized with GRSF1, a component of the mitochondrial RNA granules described previously (Figure 2B). However, BrU incorporation and mitochondrial RNA granule formation occurred normally in FASTK-depleted cells

(C) Subcellular fractionation of 143B cells and analysis by western blotting shows a lower-molecular-weight isoform of FASTK present in mitochondria. Membranes were probed with antibodies directed against FASTK, and the purity of the subcellular fractions was assessed using a cytosolic marker HSP90β, a nuclear marker P54, and a mitochondrial marker mtSSB. Additional isoforms and modification of FASTK in the nucleus or the cytosol were not investigated here.

(D) Immunoblot analysis of total isolated 143B mitochondria (T), or supernatant (S) and pellet (P) fractions after Na_2CO_3 (pH 11) extraction and ultra-centrifugation. Immunoblots were probed with antibodies against FASTK, PHB (a membrane marker), or cytochrome c (Cyt *c*, a soluble marker).

(E) Immunoblot analysis of isolated 143B mitochondria after the proteinase K accessibility test. Mitochondria were left untreated, swollen to rupture the outer membrane, or lysed in Triton X-100 prior to treatment with proteinase K. Immunoblots were probed with anti-FASTK, anti-OPA1 (an inter-membrane space protein), anti-Tom20 (a mitochondrial outer membrane protein), and anti-mtSSB (a matrix protein).

(F) Immunoblot analysis of 143B cells stably expressing FASTK-HA, FASTK-HA M35G (cytoFASTK), or FASTK-HA Δ1–34 (mitoFASTK). Membranes were probed with anti-HA antibody and then reprobed with anti-actin as a loading control

(G) Confocal microscopy of cells described in (F). Arrowheads indicate mitochondrial RNA granules.

(H) The FASTK gene showing the exon structure (1–10) and two ATG start sites at position 1, coding for methionine 1 (M1) and at position 103, coding for methionine 35 (M35). FASTK protein can be translated from either site, but the mitochondrial targeting signal (M) of FASTK is exposed only when translation starts at ATG 103. FAST_1, FAST_2, and RAP are the conserved domains of FASTK.

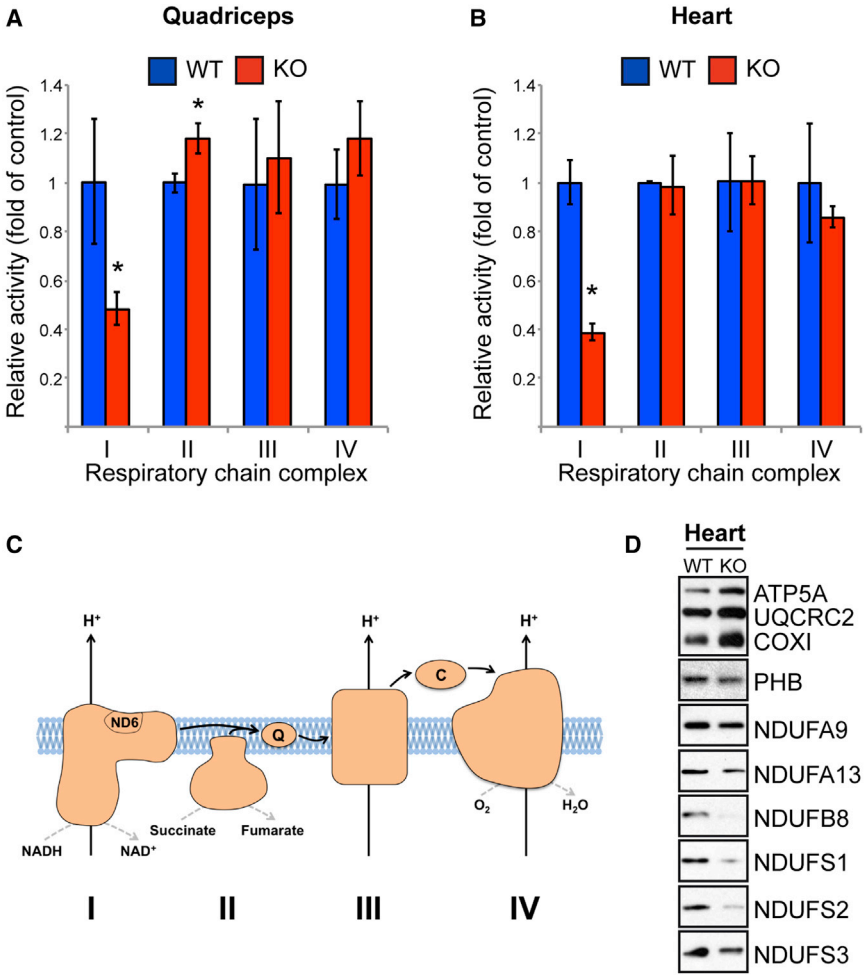

Figure 3. FASTK Is Required for NADH Complex Activity

(A) Analysis of mitochondrial enzymatic activity on quadriceps from FASTK$^{+/+}$ (WT) and FASTK$^{-/-}$ (KO) mice. Enzymatic activities were normalized to the citrate synthase activity. Data from three different mice are represented as mean ± SEM. *$p < 0.05$ using a Mann-Whitney test; $n = 3$.

(B) A similar analysis to that shown in (A) was performed on mouse hearts.

(C) Schematic representation of the mitochondrial electron transport chain: I, NADH dehydrogenase complex; II, succinate dehydrogenase complex; III, cytochrome bc_1 complex; IV, cytochrome *c* oxidase complex. Q, ubiquinone/ubiquinol; C, cytochrome *c*.

(D) Immunoblot analysis of FASTK$^{+/+}$ (WT) and FASTK$^{-/-}$ (KO) hearts with the indicated antibodies.

(Figure S3A), suggesting that FASTK is not an essential structural component of the mitochondrial RNA granules. Of the other members of the FASTK family, only FASTKD2 co-localized with BrU foci (Figure 2B) whereas no co-localization with RNA granules was observed for FASTKD1, FASTKD3, FASTKD4 (TBRG4), or FASTKD5 (Figure S3B). Together, these data indicate that the mitochondrial isoform of FASTK is a component of mitochondrial RNA granules and that it is not required for maintaining their structural integrity. The role of FASTKD2 in mitochondrial RNA granules will be reported elsewhere.

FASTK Is Required for Mitochondrial NADH Dehydrogenase Activity

To test whether FASTK plays a role in mitochondrial function, we took advantage of existing mice with a disrupted FASTK gene (Simarro et al., 2010a). We first tested the enzymatic activity of the respiratory chain complexes from the skeletal and cardiac muscles of FASTK$^{+/+}$ and FASTK$^{-/-}$ animals and observed an ~60% decrease in mitochondrial NADH dehydrogenase (complex I) activity in both tissues, whereas the activity of other complexes was not significantly altered or was even slightly increased (Figures 3A–3C). The specific complex I deficiency was confirmed by oxygraphy using two independent FASTK$^{+/+}$ and two independent FASTK$^{-/-}$ MEF lines (Figure S4). Protein immunoblot analysis showed that the steady-state levels of several subunits of complex I, including NDUFB8, NDUFS1, and NDUFS2, were decreased in the heart of FASTK$^{-/-}$ animals, suggesting a partial disassembly of the complex as previously described (Heide et al., 2012; Karamanlidis et al., 2013), whereas subunits of the other complexes were normally expressed (Figure 3D). Thus, these results indicate that FASTK is specifically required for mitochondrial NADH dehydrogenase activity both in vitro and in vivo.

FASTK Specifically Regulates ND6 mRNA Levels

Because FASTK is thought to bind RNA and is localized in the mitochondrial RNA granules as shown above, we reasoned that it may play a role in the post-transcriptional regulation of mtDNA-encoded subunit(s) of the respiratory complex I. We therefore performed a northern blot analysis to compare the expression of these mRNAs in wild-type and FASTK$^{-/-}$ cells. MEFs isolated from FASTK$^{-/-}$ animals showed a dramatic reduction in the level of ND6 mRNA (*MTND6*), which encodes subunit 6 of the NADH dehydrogenase complex, whereas all other subunits of complex I were normally expressed (Figure 4A). Importantly, reintroduction of human mitoFASTK, but not cytoFASTK, into FASTK$^{-/-}$ MEFs restored *MTND6* levels, indicating that the regulation of *MTND6* is under the control of the mitochondrial form of FASTK (Figure 4B). We confirmed the depletion of *MTND6* in the brain, heart, muscle, and liver from FASTK$^{-/-}$ mice (Figure 4C). Similar results were obtained using 143B cells in which FASTK was depleted by RNAi (Figure 4D). The level of all other mtDNA-encoded RNAs, including the other 12 ORFs, was within the control range or slightly

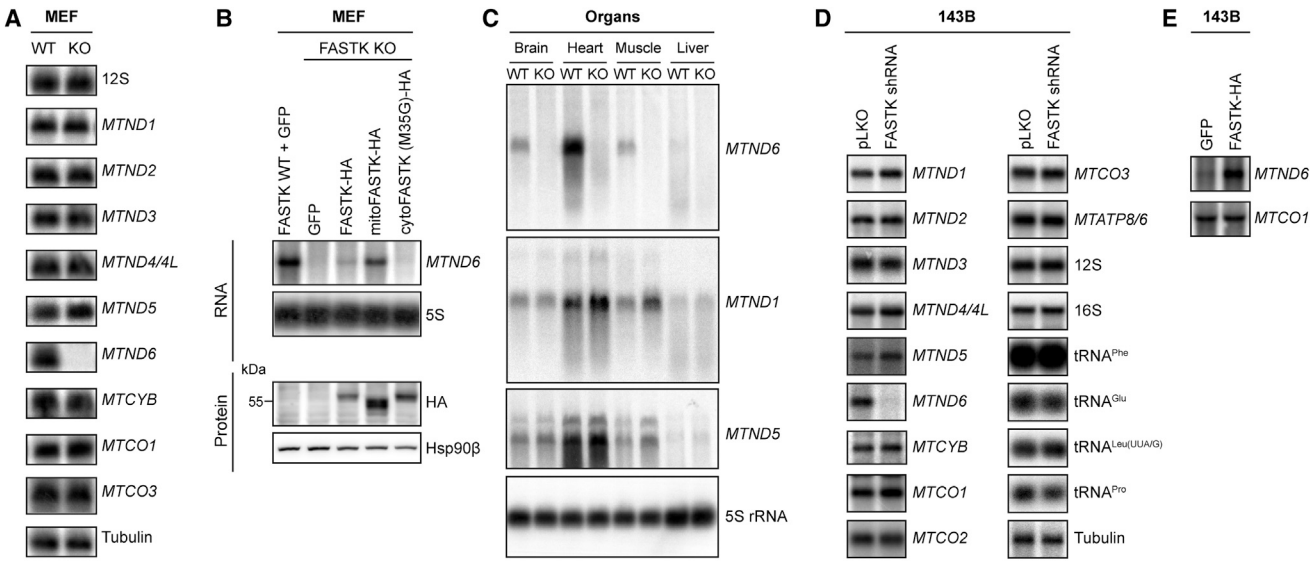

Figure 4. FASTK Regulates ND6 mRNA Expression in Mitochondria

(A) Northern blot analysis of total RNA from FASTK$^{+/+}$ (WT) and FASTK$^{-/-}$ (KO) MEFs using riboprobes against all mitochondrial-encoded subunits of complex I.

(B) Northern blot and immunoblot analysis of FASTK$^{+/+}$ (WT) and FASTK$^{-/-}$ (KO) MEFs, in which GFP, FASTK-HA, mitoFASTK-HA (Δ1–34), or cytoFASTK-HA (M35G) have been stably introduced.

(C) Northern blot analysis of total RNA from four different organs of FASTK$^{+/+}$ (WT) and FASTK$^{-/-}$ (KO) mice probed for the sequences indicated.

(D) Northern blot analysis of total RNA from 143B cells stably expressing an shRNA against FASTK, or the empty vector (pLKO), probed for the sequences indicated.

(E) Northern blot analysis of total RNA from 143B cells stably expressing GFP or FASTK-HA using riboprobes directed against *MTND6* or *MTCO1*.

higher in FASTK-depleted cells and animals (Figures 4A, 4C, and 4D). Strikingly, overexpression of human FASTK-HA in 143B cells led to the strong stabilization of ND6 mRNA, indicating that FASTK is a limiting factor in the regulation of *MTND6* expression (Figure 4E). Taken together, our results indicate that FASTK specifically controls the expression of ND6 mRNA in both cultured cells and mice.

The RAP Domain of FASTK Plays a Central Role in the Regulation of ND6 mRNA

Among the conserved domains of the FASTK family, the RAP domain has been predicted to bind RNA (Lee and Hong, 2004; Figure 5A). This may explain the presence of the FASTK family members in recent studies that identified mRNA-interacting proteins (Baltz et al., 2012; Castello et al., 2012). Our data thus far have demonstrated that FASTK regulates *MTND6*; therefore, we investigated whether the two molecules could interact and whether such an interaction may involve the RAP domain. For this, we first generated 143B cells that stably expressed mitoFASTK-HA and used these cells to perform immunoprecipitation experiments using an antibody directed against the HA tag. The immunoprecipitated RNAs were analyzed by dot-blotting (RNA-IP) using riboprobes specific for *MTND6* and several other mitochondrial-encoded RNAs. As shown in Figure 5C (left panel), we found that *MTND6* was specifically enriched in the mitoFASTK-HA immunoprecipitate, whereas none of the other mitochondrial RNAs were detected. To test the role of the RAP domain in mediating the interaction between FASTK and *MTND6*, we generated a second line of 143B cells that stably expressed a mitoFASTK mutant lacking the RAP domain (mitoFASTKΔRAP-HA). mitoFASTKΔRAP-HA expression did not prevent the incorporation of BrU into newly synthesized RNA (Figure S3A). RNA-IP using these cells revealed that the interaction of *MTND6* with mutant FASTK was greatly reduced compared to wild-type mitoFASTK (Figure 5C, right panel), even though both versions of mitoFASTK were efficiently and selectively precipitated by the anti-HA antibodies (Figure 5B). When introduced into FASTK$^{-/-}$ MEFs or into 143B cells depleted of FASTK, mitoFASTKΔRAP-HA could enter mitochondria (Figure 5E) but did not localize to mitochondrial RNA granules and was not able to restore *MTND6* expression (Figure 5D). Thus, we conclude that FASTK interacts with *MTND6* and that the RAP domain is essential for this interaction. Deletion of the RAP domain results in loss of the ND6-processing function of FASTK and loss of its association with mitochondrial RNA granules.

The Mature ND6 mRNA Contains a 3′ UTR

MTND6 is the only mRNA encoded by the light strand. The 5′ end of the protein-coding sequence is flanked by tRNA^{Glu} (Figure S5A). However, there is no flanking downstream tRNA, and the processing of its 3′ end is thus an exception to the tRNA punctuation model (Ojala et al., 1980). Instead, ND6 mRNA is adjacent to a long stretch of non-coding RNA that is complementary to ND5 and is sometimes referred to as "mirror" ND5 (Figure S5A). Indeed, there is no clear agreement regarding the length of *MTND6* 3′ UTR: whereas the original publication describing this mRNA reported a coding sequence of 525 nucleotides followed by a 3′ UTR of 500–600 nucleotides (Ojala et al., 1980; Tullo

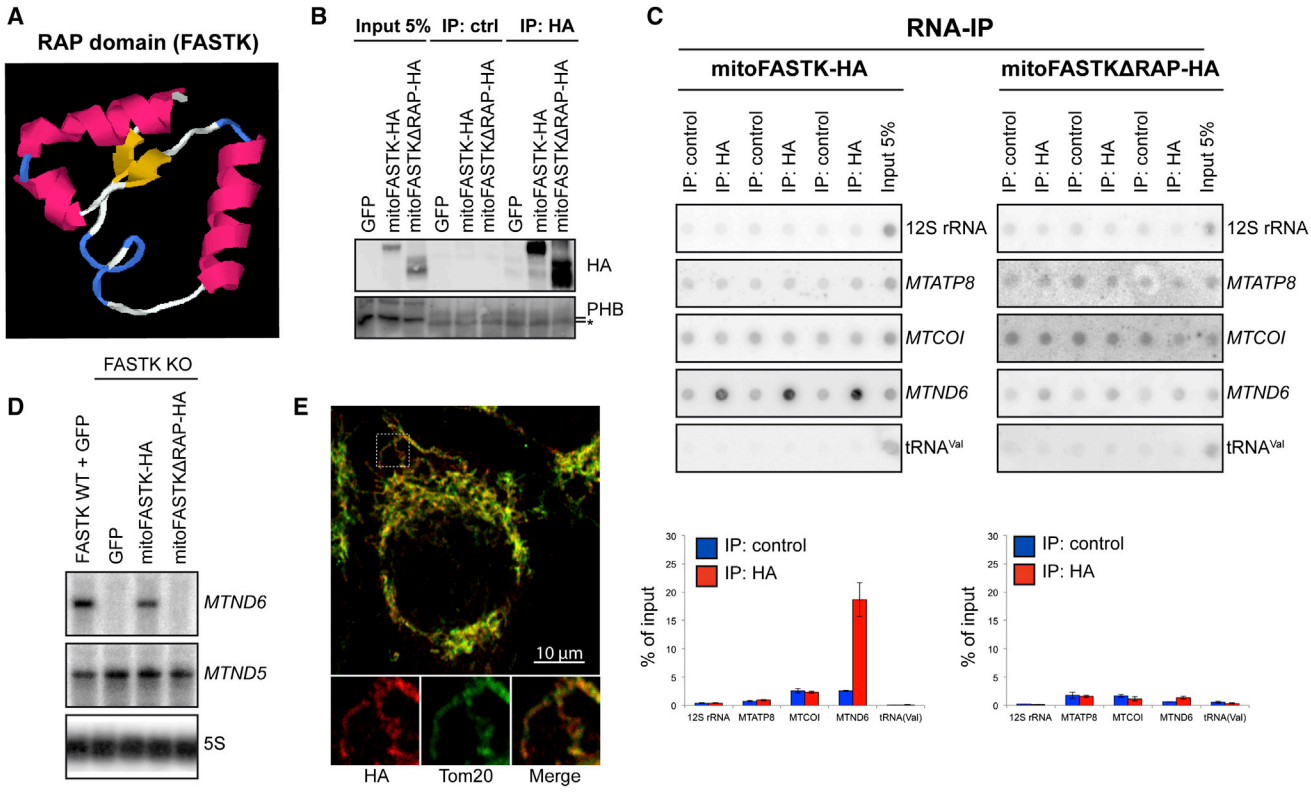

Figure 5. The RAP Domain of FASTK Is Required for Binding to ND6 mRNA and for FASTK Localization and Function

(A) Structural prediction of the RAP domain from FASTK according to I-TASSER. Details are given in Figure S1.

(B) Immunoblot analysis after immunoprecipitation with rabbit polyclonal antibodies directed against HA or FLAG (ctrl). Mitochondrial lysates for immunoprecipitation were prepared from 143B cells expressing GFP, mitoFASTK-HA, or mitoFASTK-ΔRAP-HA. PHB was used as a negative control. * indicates the IgG light chain.

(C) RNA dot blot and quantification after immunoprecipitation as described in (B). Exposures shown here are made so that the "input" signal is comparable between the different probes. Data are represented as mean ± SEM. n = 3.

(D) Northern blot analysis of FASTK$^{+/+}$ (WT) and FASTK$^{-/-}$ (KO) MEFs in which GFP, FASTK-HA, mitoFASTK-HA, or mitoFASTK-ΔRAP-HA have been stably introduced.

(E) Confocal microscopy of 143B cells stably expressing mitoFASTK-ΔRAP-HA immunostained with antibodies directed against HA or Tom20, a mitochondrial marker.

et al., 1994; Slomovic et al., 2005; Ruzzenente et al., 2012), others have reported that the 3′ UTR of ND6 is only 33 to 34 nucleotides (Mercer et al., 2011). We therefore decided to reassess this question. Northern blots from wild-type and ρ^0 cells were probed with riboprobes directed against the coding sequence of ND6 (riboprobe: CDS) or against its putative long 3′ UTR (riboprobe: UTR). Both probes revealed the same major transcript of 1.0–1.1 kb consistent with the original report, whereas several higher-molecular-weight transcripts could also be discerned that were absent in RNA from ρ^0 cells (Figure S5B, black arrows).

FASTK Binds at Multiple Sites within the ND6 mRNA Precursor

Because FASTK is enriched in mitochondrial RNA granules, the sites at which the newly synthesized RNAs are concentrated, we wished to know whether FASTK could interact directly with the ND6 mRNA and/or its precursors during *MTND6* biogenesis. First, to determine whether loss of FASTK affects the expression of light-strand-encoded genes other than ND6, we performed northern blotting using probes against tRNA^{Pro}, tRNA^{Glu}, mirror ND4/4L, or mirror COI (Figures 4D and S5C). No difference was seen in the level of any of these transcripts in cells depleted for FASTK, indicating that FASTK does not play a general role in light-strand RNA metabolism. It is particularly noteworthy that the level of tRNA^{Glu} immediately upstream of ND6 is unaffected (Figures 4D and S5D), which implies that FASTK does not participate in 5′ end processing of *MTND6*. To study processing of the 3′ end of *MTND6*, northern blots were exposed to a probe directed against the non-coding RNA region corresponding to mirror ND5 (Figures S5A and S5B). This probe revealed several higher-molecular-weight species present at low levels and possibly related to the higher-molecular-weight RNAs revealed by the two ND6-specific probes (Figure S5B, arrows). These RNAs likely represent the ND6 precursors described in the original study and referred to as RNAs 1–3 (Ojala et al., 1980; Figure 6C, bottom). This therefore prompted us to test whether FASTK could bind any of the ND6 precursors. To answer this question, we repeated the RNA-IP as described in Figure 5

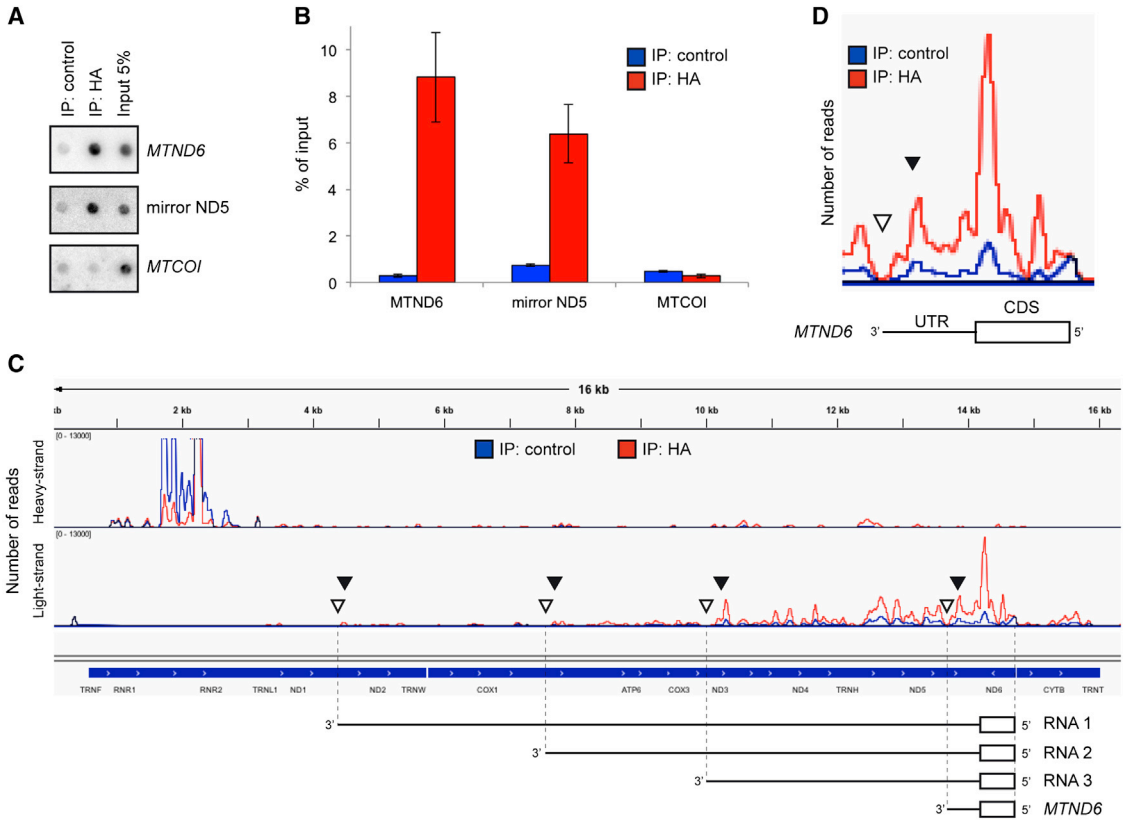

Figure 6. FASTK Binds the Precursors of ND6 mRNA

(A) RNA dot blot after immunoprecipitation using probes directed against *MTND6*, mirror ND5, or MTCO1. The RNA-IP was performed in RNase-free conditions. Exposures shown here are made so that the "input" signal is comparable between the different probes.

(B) Phosphorimager quantification of the data shown in (A). Data are represented as mean ± SEM. n = 3.

(C) IGV view of the RNA fragments bound to FASTK and aligned to the mitochondrial genome. The RNA-IP was partially digested with RNase I and sequenced using next-generation RNA sequencing. Essentially no enrichment for heavy-strand transcripts was observed (rRNAs are considered as contaminants and are enriched to the same extent in both IPs). In contrast, a strong enrichment of light-strand-encoded RNAs was observed specifically in the region encoding the ND6 transcripts. These results confirm the dot blotting shown in (A). Black arrowheads indicate sites of increased protection at the 3′ ends of the ND6 mRNA and precursor RNAs 1, 2, and 3 in the regions immediately preceding the 3′ processing site. White arrowheads indicate the 3′ processing sites for ND6 mRNA and RNAs 1, 2, and 3, all of which are devoid of FASTK-mediated protection. Bottom: schematic representation of the mature ND6 mRNA and precursor RNAs 1–3. Rectangles represent the ND6 coding sequence; lines represent non-coding sequences.

(D) Detailed view of the region corresponding to ND6 mRNA in (C). CDS: coding sequence. UTR: untranslated region.

and probed the dot blots with the downstream mirror ND5 riboprobe. A significant increase in the signal was found in the mito-FASTK-HA immunoprecipitate, indicating that FASTK binds to, and is able to immunoprecipitate, the precursors of ND6 mRNA (Figures 6A and 6B). In order to refine our analysis of the region bound by FASTK within the precursor RNA, we repeated the RNA-IP and then performed a partial digestion with RNase I and analyzed the protected RNA fragments using next-generation RNA sequencing. Alignment of the sequences obtained to the mitochondrial genome is shown in Figure 6C. Apart from the presence of highly abundant rRNAs that are also seen in the negative control, the results show that most of the protected RNA fragments are transcribed from the DNA light strand. No enrichment for heavy-strand RNAs was observed (Figure 6C). The protected sequences covered the coding sequence of ND6 mRNA, its 3′ UTR, and to a lesser extent the downstream sequences (Figures 6C and 6D).

FASTK Modulates Degradosome Activity to Generate the Mature ND6 mRNA

We next wished to investigate the RNase activity responsible for depletion of *MTND6* in the absence of FASTK. Light-strand non-coding RNAs, or "mirror" RNAs, are normally eliminated by the mitochondrial degradosome, which is composed of the helicase hSuv3p, and the polynucleotide phosphorylase PNPase, a 3′-5′ exoribonuclease (Borowski et al., 2013). Interestingly, both the PNPase and hSuv3p are found in mitochondrial RNA granules (Borowski et al., 2013). Because *MTND6* is encoded on the light strand, we reasoned that this mRNA could also be a substrate for the degradosome, and we therefore wished to investigate whether, in the absence of FASTK, the degradosome could be responsible for the complete elimination of *MTND6*. As previously reported, we found that downregulation of either the PNPase or hSuv3p led to the accumulation of mirror COI and mirror ND4/4L, whereas the

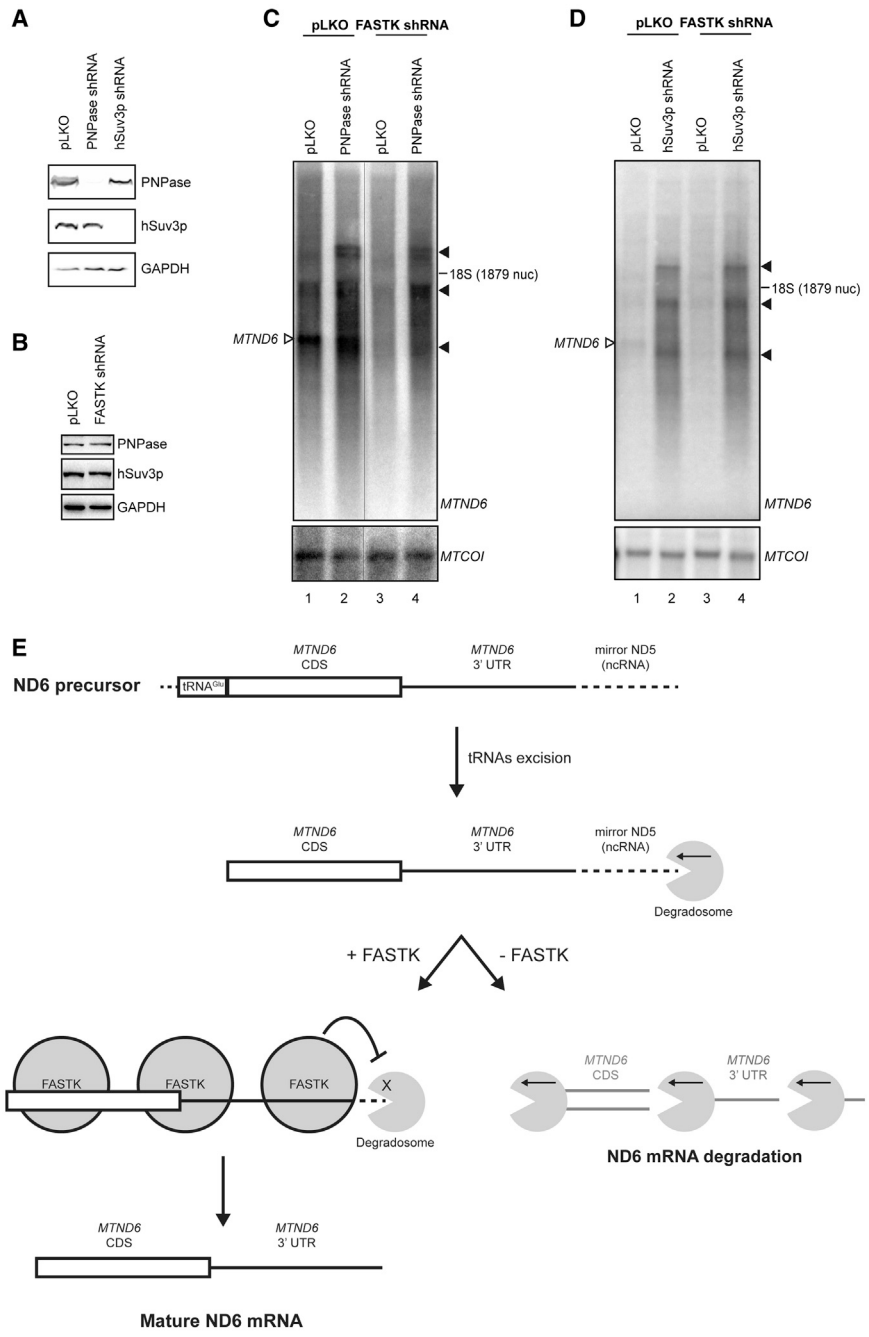

Figure 7. FASTK Modulates Degradosome Activity to Generate the Mature ND6 mRNA

(A) Immunoblot analysis of 143B cells stably expressing an shRNA against either PNPase or hSuv3p and probed with antibodies directed against PNPase, hSuv3p, or GAPDH. pLKO corresponds to the empty vector.

(B) Immunoblot analysis of 143B cells stably expressing an shRNA against FASTK probed with antibodies directed against the PNPase, hSuv3p, or GAPDH. pLKO corresponds to the empty vector.

(C) Northern blot analysis of cells stably expressing shRNAs against FASTK and/or the PNPase. Parallel blots were probed to reveal *MTND6* or *MTCO1*. White arrowhead, mature *MTND6*. Black arrowheads, *MTND6*-containing RNAs. pLKO corresponds to the empty vector.

(D) Northern blot analysis of cells stably expressing shRNAs against FASTK and/or hSuv3p. Parallel blots were probed to reveal *MTND6* and *MTCO1*. White arrowhead, mature *MTND6*. Black arrowheads, *MTND6*-containing RNAs. pLKO corresponds to the empty vector.

(E) Proposed mechanism in which FASTK binds the precursor forms of ND6 mRNA at multiple sites, including the 3′ UTR, and prevents its degradation during processing of the light strand by the mitochondrial degradosome. In the absence of FASTK, uncontrolled activity of the degradosome leads to complete elimination of the entire ND6 mRNA (see Discussion for more details). CDS: coding sequence. UTR: untranslated region. ncNA: non-coding RNA.

heavy-strand transcripts, *MTCOI* and 12S, were not at all or only mildly affected (Figures 7C, 7D, and S5C). Interestingly, depletion of either component of the degradosome also led to the strong accumulation of ND6-containing transcripts (Figures 7C and 7D lines 1 and 2, black arrowheads), suggesting that the degradosome is also involved in the generation of *MTND6*. To find out whether activity of the degradosome could be responsible for the loss of *MTND6* in the absence of FASTK, we depleted both FASTK and the PNPase or hSuv3p. As expected, *MTND6* was not detected in cells depleted for FASTK alone. However, when the degradosome activity was also impaired, we found a considerable increase in ND6-containing transcripts of various sizes, although significantly no accumulation of mature *MTND6*, indicating that the degradosome is responsible for *MTND6* degradation in the absence of FASTK. In control experiments, we showed that the abundance of the degradosome subunits was not affected by the depletion of FASTK (Figure 7B). Based on these data, we conclude that the degradosome participates in the processing of the light-strand-encoded RNAs and is largely responsible for the depletion of *MTND6* in the absence of FASTK.

DISCUSSION

In this report, we have studied the RNA-binding protein FASTK, a protein previously found to be associated with RNA granules in the nucleus and cytoplasm. Here, we report the existence of a translational variant of FASTK that is targeted to mitochondria, where it co-localizes with the mitochondrial RNA granules. We provide evidence that the

mitochondrial form of FASTK binds ND6 mRNA and its precursors and that it cooperates with the mitochondrial degradosome to regulate ND6 mRNA biogenesis. Accordingly, we found that depletion of FASTK results in the loss of mature ND6 mRNA, leading to reduced complex I activity in both cultured cells and mice.

Regulation of ND6 mRNA Biogenesis by the Mitochondrial Isoform of FASTK

FASTK was previously reported to localize to speckles in the nucleus and to P-bodies and stress granules in the cytoplasm (Kedersha et al., 2005; Simarro et al., 2007). We have now identified a second translation initiation site in the FASTK mRNA immediately upstream of a cryptic MTS. Use of this alternative start site generates a shorter protein that is localized to mitochondria, where it concentrates in the mitochondrial RNA granules. The existence of a cryptic MTS is not exclusive to FASTK, and similar sequences have recently been described for several other proteins (Kazak et al., 2013), suggesting that internal initiation of translation upstream of a specific targeting sequence may provide a general mechanism by which a single mRNA is able to generate different isoforms destined for localization to distinct subcellular compartments.

We report that the mitochondrial form of FASTK is involved specifically in the regulation of ND6 mRNA. Interestingly, whereas depletion of FASTK resulted in loss of *MTND6*, overexpression of the protein led to significant increase in this mRNA compared to control cells (Figure 4E), suggesting that binding to FASTK is a rate-limiting step in the control of ND6 mRNA levels. *MTND6* is unique in being the only protein-coding transcript encoded on the light strand of the mitochondrial genome. It is also an exception to the tRNA punctuation model, because there is no tRNA adjacent to the 3′ end of the coding sequence, and indeed *MTND6* is one of the rare mitochondrial RNAs that has an extended 3′ UTR and that, at steady state, also exists in the form of several higher-molecular-weight precursors previously referred to as RNAs 1–3 (Ojala et al., 1981). Our analysis of the RNA sequences bound to FASTK following partial RNase digestion showed that FASTK binds specifically light-strand-encoded RNAs and protects in particular the ND6 mRNA-coding sequence and its 3′ UTR (Figure 6D). Very little is known about the processing of the light-strand precursor RNA, which also contains the non-coding so-called "mirror" sequences. In previous work, it was reported that the mirror RNAs are degraded by the degradosome and that they accumulate when either the PNPase or the helicase hSuv3p components of the degradosome are depleted (Szczesny et al., 2010; Borowski et al., 2013). We have confirmed these results and have extended our analysis of degradosome activity to include its role in expression of *MTND6*. We observed that *MTND6*-containing transcripts also accumulate in the absence of PNPase or hSuv3p (Figures 7C and 7D), indicating that, like the mirror RNAs, *MTND6* levels are regulated by the degradosome. Mitochondrial mRNAs encoded on the heavy strand, however, such as *MTCOI*, were insensitive to depletion of the degradosome (Figure S5C). Strikingly, in cells depleted for FASTK, we could restore expression of *MTND6*-containing transcripts by depletion of PNPase or hSuv3p (Figures 7C and 7D, lanes 3 and 4). However, in this case, we observed no enrichment for the 1.0–1.1 kb transcript corresponding to the mature ND6 mRNA. This result suggests first that FASTK protects *MTND6* from the degradosome and second that it is involved in defining the length of the mature mRNA. Taken together with the observations that (1) only the 5′ end of the ND6 mRNA is defined by tRNA excision; (2) FASTK binds at multiple sites along *MTND6*, and (3) the region downstream of ND6 encodes "mirror" RNAs that are normally eliminated by the degradosome, we have proposed a model shown in Figure 7E, in which binding to FASTK defines the length and the abundance of *MTND6* by regulating the processing activity of the degradosome. Thus, in the absence of FASTK, the unbound ND6 mRNA is completely eliminated by the degradosome, whereas in the absence of both FASTK and an active degradosome, high-molecular-weight, ND6-containing precursor RNAs accumulate, although the mature ND6 mRNA of 1.0–1.1 kb is not generated. We propose that binding of FASTK is a rate-limiting step in controlling the abundance of *MTND6* because its depletion leads to loss of *MTND6* and its overexpression results in the stabilization of this mRNA (Figure 4). A similar process has recently been described in chloroplasts where certain pentatricopeptide-repeat (PPR) proteins participate in a "barrier" mechanism in which the protein binds directly to the 3′ end of a mRNA, blocking its degradation by the 3′-5′ PNPase activity (Barkan and Small, 2014). Although several PPR proteins have been identified in human mitochondria, including POLRMT or the PTCD1–3, to our knowledge none of them play a role in the stability of *MTND6*. On the other hand, FASTK is predicted to share a similar global architecture to PPR proteins, including the repeated α helix motifs (Figure S1B), and indeed FASTK has previously been referred to as an "octotricopeptide-repeat" (OPR) protein (Eberhard et al., 2011). Furthermore, it is interesting that a RAP-domain-containing protein has very recently been identified in chloroplasts of *Arabidopsis*, which, in a manner analogous to FASTK, has been shown to bind to and regulate the processing of the 12S rRNA (Kleinknecht et al., 2014). Thus, in widely divergent species, FASTK and FASTK-related proteins appear to be part of a conserved mechanism involved in the biogenesis of organellar RNAs.

Functional Relevance of the Loss of FASTK

The ND6 protein is thought to be a key component of the respiratory chain complex I because a nonsense mutation in this gene leads to complex I disassembly (Bai and Attardi, 1998). In agreement with these findings, we found an ~60% loss of complex I activity in different tissues from FASTK$^{-/-}$ animals (Figures 3A and 3B), and this was accompanied by a concomitant decrease in the level of several nuclear-encoded subunits of complex I (Figure 3D), also indicating a partial disassembly of the complex. The decrease in NADH dehydrogenase activity however was not as strong as we might have expected from the dramatic depletion of ND6 mRNA. This could indicate either that ND6 does not play the critical role in complex I assembly that had been previously proposed (Deng et al., 2006) or that low-level residual ND6 mRNA is able to produce sufficient ND6 protein to permit some complex I activity (Perales-Clemente et al., 2011). Unfortunately, in the absence of good commercially available antibodies against ND6 (Perales-Clemente et al., 2011), we have

not been able to distinguish between these possibilities in our experiments.

In conclusion, we have described a novel component of the mitochondrial RNA granules, FASTK, which is essential for *MTND6* expression. We propose a model that predicts that binding of FASTK to the *MTND6* transcript blocks the activity of the degradosome and participates in delineating its 3′ end. Intriguingly, FASTK is localized in several other types of RNA granules, including P-bodies and stress granules that appear to play diverse roles in post-transcriptional regulation of mRNA, including mRNA modification and degradation (Anderson and Kedersha, 2009). It is tempting to speculate that similar processes occur in the mitochondrial RNA granules where FASTK ensures the regulated expression of the ND6 mRNA.

EXPERIMENTAL PROCEDURES

Cell Culture and Transfection

All cell culture reagents were from GE Healthcare. Cells were cultured in DMEM supplemented with 10% heat-inactivated fetal bovine serum, 100 u/ml penicillin, 100 μg/ml streptomycin, and 2 mM L-glutamine. When 143B ρ^0 were used, the culture medium was further supplemented with 110 μg/ml pyruvate and 50 μg/ml uridine. Transfections were performed using calcium phosphate or Fugene (Roche).

Bromouridine Staining, Immunofluorescence, and Microscopy

BrU staining, immunofluorescence, and microscopy were performed as previously described (Jourdain et al., 2013). Briefly, BrU staining was performed by incubating cells for 1 hr with 5 mM BrU (Sigma-Aldrich) and immunostaining with anti-BrU/BrdU (Roche) was performed in PBS containing 0.1% Triton X-100 and 3% w/v BSA (Sigma-Aldrich). Imaging was performed using a Zeiss LSM700 confocal microscope. All antibodies used are described in Table S1.

RNA Extraction and Northern Blotting

RNA extraction and northern blot analyses were performed as previously described (Jourdain et al., 2013). Briefly, total RNA was extracted with Tri Reagent (Sigma-Aldrich) and GlycoBlue (Ambion). 5–15 μg RNA were separated on a denaturing formaldehyde agarose gel and transferred electrophoretically to a Nylon membrane (GE Healthcare). Strand-specific radiolabelled riboprobes (Table S1) were transcribed in vitro using T7 polymerase (Bio-Rad) in the presence of ^{32}P-UTP, and hybridization was performed at 60°C in 50% formamide, 7% SDS, 0.2M NaCl, 80 mM sodium phosphate (pH 7.4), and 100 μg/ml salmon sperm DNA. Imaging was done with a phosphorimager (Bio-Rad).

Mitochondria-Rich Fraction Isolation, Protein Import, Proteinase K Accessibility Test, and Alkali Treatment

Preparation of cytosolic, nuclear, and mitochondria-rich fractions; protein import assays; proteinase K accessibility testing; and alkali treatment were performed as described previously (Jourdain et al., 2013).

Immunoprecipitation, Partial RNase Digestion, and RNA Sequencing

A mitochondria-rich fraction was isolated form 143B cells stably expressing a C-terminal tagged version of the gene of interest and resuspended in IP buffer (50 mM Tris/HCl [pH 7.5], 150 mM NaCl, 1 mM MgCl2, 1% NP-40, 3 mM vanadylate RNase complex, and 400 u/ml RNAsin Plus [Promega]). Protein-G-coated Dynabeads (Invitrogen) were washed and incubated in the same buffer with polyclonal anti-HA (Abcam) or polyclonal anti-FLAG (Sigma-Aldrich). Beads were then washed, the mitochondrial lysate was added, and the mixture was incubated overnight at 4°C. For partial RNase treatment, beads were washed twice and incubated for 5 min at 37°C with 0.2 u/μl of RNase I (Ambion) in IP buffer without RNase, vanadylate, and RNAsin. After extensive washing, the tubes were changed and the digested RNAs were 3′ dephosphorylated on beads for 20 min at 37°C using polynucleotide kinase (PNK; Promega) in absence of ATP. 5′ phosphorylation was achieved by incubating the RNAs with PNK in presence of ATP for 10 min according to the manufacturer's instructions, before RNA extraction. Quality control, RNA size profiling to ensure correct RNase I digestion, library preparation, and Illumina MiSeq 1 × 50 sequencing were performed at Fasteris (Plan-les-Ouates). Sequences were mapped to the human genome (hg38) using Bowtie. The sequences were aligned to the human mitochondrial genome (NC_012920), visualized and quantified with IGV (Broad Institute).

Cloning, Viral Production, and RNAi

For protein expression, cDNAs were cloned in pCi (Promega) in frame with a C-terminal HA-TEV-6HIS tag. Primers are described in Table S1. cDNAs were then subcloned into pWPT with the following primers: fwd: ATC GAT CGA CGC GTA CTT AAT ACG ACT CAC TAT AG; rev: CGA TCG ATG TCG ACA ATG TAT CTT ATC ATG TCT GCT C using MluI and SalI restriction enzymes. Lentiviruses for protein expression were produced in 293T HEK by co-transfecting the constructs of interest cloned into the pWPT vector with the viral plasmids psPAX2 and pMD2G (Addgene). After 2 days, the supernatant was collected, filtered at 0.45 μm, and used to infect 143B cells. shRNA sequences were supplied precloned in either pLKO.1 (Sigma) or pLKO-TetON (Addgene; Table S1), and the same protocol of lentivirus production was used. After infection for >24 hr, cells were selected with 3 μg/ml puromycin (Sigma) overnight and were analyzed >24 hr after addition of puromycin. pLKO-TetON is a tetracycline-inducible version of pLKO.1 and was induced with 1 μg/ml of doxycycline for 3–5 days. pLKO.1 or pLKO-TetON empty vectors were always included as negative controls.

Mitochondrial Enzymatic Activities and Respiration Rates

Please refer to the Supplemental Experimental Procedures.

SUPPLEMENTAL INFORMATION

Supplemental Information includes Supplemental Experimental Procedures, five figures, and one table and can be found with this article online at http://dx.doi.org/10.1016/j.celrep.2015.01.063.

ACKNOWLEDGMENTS

We would like to thank Y. Brixner and S. Montessuit for their technical support, all members of the J.-C.M. lab for their comments on the manuscript, and M. Zeviani, C. Viscomi, Z. Chrzanowska-Lightowlers, R.N. Lightowlers, M. Goldschmidt-Clermont, S. Thore, D. Martinvalet, G. Voeltz, D. Picard, F. Stutz, and their laboratories for sharing reagents and for intellectual input during the project. This work was supported by the Swiss National Science Foundation (31993A-141068/1), IGE3, and the State of Geneva. MS work was supported by the Gerencia Regional de Salud de la JCyL (GRS 642/A/11) and Roche Diagnostics.

Received: July 8, 2014
Revised: December 10, 2014
Accepted: January 29, 2015
Published: February 19, 2015

REFERENCES

Anderson, P., and Kedersha, N. (2009). RNA granules: post-transcriptional and epigenetic modulators of gene expression. Nat. Rev. Mol. Cell Biol. *10*, 430–436.

Antonicka, H., Sasarman, F., Nishimura, T., Paupe, V., and Shoubridge, E.A. (2013). The mitochondrial RNA-binding protein GRSF1 localizes to RNA granules and is required for posttranscriptional mitochondrial gene expression. Cell Metab. *17*, 386–398.

Bai, Y., and Attardi, G. (1998). The mtDNA-encoded ND6 subunit of mitochondrial NADH dehydrogenase is essential for the assembly of the membrane arm and the respiratory function of the enzyme. EMBO J. *17*, 4848–4858.

Baltz, A.G., Munschauer, M., Schwanhäusser, B., Vasile, A., Murakawa, Y., Schueler, M., Youngs, N., Penfold-Brown, D., Drew, K., Milek, M., et al. (2012). The mRNA-bound proteome and its global occupancy profile on protein-coding transcripts. Mol. Cell *46*, 674–690.

Barkan, A., and Small, I. (2014). Pentatricopeptide repeat proteins in plants. Annu. Rev. Plant Biol. *65*, 415–442.

Bogenhagen, D.F., Martin, D.W., and Koller, A. (2014). Initial steps in RNA processing and ribosome assembly occur at mitochondrial DNA nucleoids. Cell Metab. *19*, 618–629.

Borowski, L.S., Dziembowski, A., Hejnowicz, M.S., Stepien, P.P., and Szczesny, R.J. (2013). Human mitochondrial RNA decay mediated by PNPase-hSuv3 complex takes place in distinct foci. Nucleic Acids Res. *41*, 1223–1240.

Castello, A., Fischer, B., Eichelbaum, K., Horos, R., Beckmann, B.M., Strein, C., Davey, N.E., Humphreys, D.T., Preiss, T., Steinmetz, L.M., et al. (2012). Insights into RNA biology from an atlas of mammalian mRNA-binding proteins. Cell *149*, 1393–1406.

Chinnery, P.F., and Hudson, G. (2013). Mitochondrial genetics. Br. Med. Bull. *106*, 135–159.

Deng, J.H., Li, Y., Park, J.S., Wu, J., Hu, P., Lechleiter, J., and Bai, Y. (2006). Nuclear suppression of mitochondrial defects in cells without the ND6 subunit. Mol. Cell. Biol. *26*, 1077–1086.

Eberhard, S., Loiselay, C., Drapier, D., Bujaldon, S., Girard-Bascou, J., Kuras, R., Choquet, Y., and Wollman, F.A. (2011). Dual functions of the nucleus-encoded factor TDA1 in trapping and translation activation of atpA transcripts in Chlamydomonas reinhardtii chloroplasts. Plant J. *67*, 1055–1066.

Ghezzi, D., Saada, A., D'Adamo, P., Fernandez-Vizarra, E., Gasparini, P., Tiranti, V., Elpeleg, O., and Zeviani, M. (2008). FASTKD2 nonsense mutation in an infantile mitochondrial encephalomyopathy associated with cytochrome c oxidase deficiency. Am. J. Hum. Genet. *83*, 415–423.

Hällberg, B.M., and Larsson, N.G. (2014). Making proteins in the powerhouse. Cell Metab. *20*, 226–240.

Heide, H., Bleier, L., Steger, M., Ackermann, J., Dröse, S., Schwamb, B., Zörnig, M., Reichert, A.S., Koch, I., Wittig, I., and Brandt, U. (2012). Complexome profiling identifies TMEM126B as a component of the mitochondrial complex I assembly complex. Cell Metab. *16*, 538–549.

Iborra, F.J., Kimura, H., and Cook, P.R. (2004). The functional organization of mitochondrial genomes in human cells. BMC Biol. *2*, 9.

Jourdain, A.A., Koppen, M., Wydro, M., Rodley, C.D., Lightowlers, R.N., Chrzanowska-Lightowlers, Z.M., and Martinou, J.C. (2013). GRSF1 regulates RNA processing in mitochondrial RNA granules. Cell Metab. *17*, 399–410.

Karamanlidis, G., Lee, C.F., Garcia-Menendez, L., Kolwicz, S.C., Jr., Suthammarak, W., Gong, G., Sedensky, M.M., Morgan, P.G., Wang, W., and Tian, R. (2013). Mitochondrial complex I deficiency increases protein acetylation and accelerates heart failure. Cell Metab. *18*, 239–250.

Kazak, L., Reyes, A., Duncan, A.L., Rorbach, J., Wood, S.R., Brea-Calvo, G., Gammage, P.A., Robinson, A.J., Minczuk, M., and Holt, I.J. (2013). Alternative translation initiation augments the human mitochondrial proteome. Nucleic Acids Res. *41*, 2354–2369.

Kedersha, N., Stoecklin, G., Ayodele, M., Yacono, P., Lykke-Andersen, J., Fritzler, M.J., Scheuner, D., Kaufman, R.J., Golan, D.E., and Anderson, P. (2005). Stress granules and processing bodies are dynamically linked sites of mRNP remodeling. J. Cell Biol. *169*, 871–884.

Kleinknecht, L., Wang, F., Stübe, R., Philippar, K., Nickelsen, J., and Bohne, A.V. (2014). RAP, the sole octotricopeptide repeat protein in Arabidopsis, is required for chloroplast 16S rRNA maturation. Plant Cell *26*, 777–787.

Lee, I., and Hong, W. (2004). RAP—a putative RNA-binding domain. Trends Biochem. Sci. *29*, 567–570.

Lee, K.W., Okot-Kotber, C., LaComb, J.F., and Bogenhagen, D.F. (2013). Mitochondrial ribosomal RNA (rRNA) methyltransferase family members are positioned to modify nascent rRNA in foci near the mitochondrial DNA nucleoid. J. Biol. Chem. *288*, 31386–31399.

Mercer, T.R., Neph, S., Dinger, M.E., Crawford, J., Smith, M.A., Shearwood, A.M., Haugen, E., Bracken, C.P., Rackham, O., Stamatoyannopoulos, J.A., et al. (2011). The human mitochondrial transcriptome. Cell *146*, 645–658.

Ojala, D., Merkel, C., Gelfand, R., and Attardi, G. (1980). The tRNA genes punctuate the reading of genetic information in human mitochondrial DNA. Cell *22*, 393–403.

Ojala, D., Montoya, J., and Attardi, G. (1981). tRNA punctuation model of RNA processing in human mitochondria. Nature *290*, 470–474.

Pagliarini, D.J., Calvo, S.E., Chang, B., Sheth, S.A., Vafai, S.B., Ong, S.E., Walford, G.A., Sugiana, C., Boneh, A., Chen, W.K., et al. (2008). A mitochondrial protein compendium elucidates complex I disease biology. Cell *134*, 112–123.

Perales-Clemente, E., Fernández-Silva, P., Acín-Pérez, R., Pérez-Martos, A., and Enríquez, J.A. (2011). Allotopic expression of mitochondrial-encoded genes in mammals: achieved goal, undemonstrated mechanism or impossible task? Nucleic Acids Res. *39*, 225–234.

Rackham, O., Mercer, T.R., and Filipovska, A. (2012). The human mitochondrial transcriptome and the RNA-binding proteins that regulate its expression. Wiley Interdiscip. Rev. RNA *3*, 675–695.

Ruzzenente, B., Metodiev, M.D., Wredenberg, A., Bratic, A., Park, C.B., Cámara, Y., Milenkovic, D., Zickermann, V., Wibom, R., Hultenby, K., et al. (2012). LRPPRC is necessary for polyadenylation and coordination of translation of mitochondrial mRNAs. EMBO J. *31*, 443–456.

Simarro, M., Mauger, D., Rhee, K., Pujana, M.A., Kedersha, N.L., Yamasaki, S., Cusick, M.E., Vidal, M., Garcia-Blanco, M.A., and Anderson, P. (2007). Fas-activated serine/threonine phosphoprotein (FAST) is a regulator of alternative splicing. Proc. Natl. Acad. Sci. USA *104*, 11370–11375.

Simarro, M., Giannattasio, G., De la Fuente, M.A., Benarafa, C., Subramanian, K.K., Ishizawar, R., Balestrieri, B., Andersson, E.M., Luo, H.R., Orduña, A., et al. (2010a). Fas-activated serine/threonine phosphoprotein promotes immune-mediated pulmonary inflammation. J. Immunol. *184*, 5325–5332.

Simarro, M., Gimenez-Cassina, A., Kedersha, N., Lazaro, J.B., Adelmant, G.O., Marto, J.A., Rhee, K., Tisdale, S., Danial, N., Benarafa, C., et al. (2010b). Fast kinase domain-containing protein 3 is a mitochondrial protein essential for cellular respiration. Biochem. Biophys. Res. Commun. *401*, 440–446.

Slomovic, S., Laufer, D., Geiger, D., and Schuster, G. (2005). Polyadenylation and degradation of human mitochondrial RNA: the prokaryotic past leaves its mark. Mol. Cell. Biol. *25*, 6427–6435.

Szczesny, R.J., Borowski, L.S., Brzezniak, L.K., Dmochowska, A., Gewartowski, K., Bartnik, E., and Stepien, P.P. (2010). Human mitochondrial RNA turnover caught in flagranti: involvement of hSuv3p helicase in RNA surveillance. Nucleic Acids Res. *38*, 279–298.

Temperley, R.J., Wydro, M., Lightowlers, R.N., and Chrzanowska-Lightowlers, Z.M. (2010). Human mitochondrial mRNAs—like members of all families, similar but different. Biochim. Biophys. Acta *1797*, 1081–1085.

Tian, Q., Taupin, J., Elledge, S., Robertson, M., and Anderson, P. (1995). Fas-activated serine/threonine kinase (FAST) phosphorylates TIA-1 during Fas-mediated apoptosis. J. Exp. Med. *182*, 865–874.

Tullo, A., Tanzariello, F., D'Erchia, A.M., Nardelli, M., Papeo, P.A., Sbisà, E., and Saccone, C. (1994). Transcription of rat mitochondrial NADH-dehydrogenase subunits. Presence of antisense and precursor RNA species. FEBS Lett. *354*, 30–36.

Vilardo, E., Nachbagauer, C., Buzet, A., Taschner, A., Holzmann, J., and Rossmanith, W. (2012). A subcomplex of human mitochondrial RNase P is a bifunctional methyltransferase—extensive moonlighting in mitochondrial tRNA biogenesis. Nucleic Acids Res. *40*, 11583–11593.

Wilson, W.C., Hornig-Do, H.T., Bruni, F., Chang, J.H., Jourdain, A.A., Martinou, J.C., Falkenberg, M., Spåhr, H., Larsson, N.G., Lewis, R.J., et al. (2014). A human mitochondrial poly(A) polymerase mutation reveals the complexities of post-transcriptional mitochondrial gene expression. Hum. Mol. Genet. *23*, 6345–6355.

Wolf, A.R., and Mootha, V.K. (2014). Functional genomic analysis of human mitochondrial RNA processing. Cell Rep. *7*, 918–931.